

AirMISR laboratory calibration and in-flight performance results

Nadine L. Chrien, Carol J. Bruegge, Barbara J. Gaitley

Jet Propulsion Laboratory, California Institute of Technology
4800 Oak Grove Dr., Pasadena, Ca. 91109

ABSTRACT

An Airborne Multi-angle Imaging SpectroRadiometer (AirMISR) instrument has been developed to assist in validation of the Earth Observing System (EOS) MISR experiment. The airborne instrument is built to the same performance specifications as MISR. Both instruments view the earth at nine discrete view angles, provide data products which are radiance scaled to Système International (SI) units, registered among the view angles, and geolocated. Whereas on-orbit MISR will acquire a global data set every nine days, the aircraft version is restricted to a target size of 9 x 11 km per aircraft run. AirMISR does, however, have the advantages of offering a means to testbed new mission procedures or camera designs, provide data sets which predate the MISR launch, and a means of returning to the laboratory to update the camera calibrations. This paper provides the AirMISR laboratory calibration results, as well as a comparison to its in-flight performance.

1. INTRODUCTION

The Multi-angle Imaging SpectroRadiometer (MISR)¹ instrument will launch aboard the first Earth Observing System spacecraft (EOS-AM1). MISR uses nine separate charge coupled device (CCD)-based pushbroom cameras to observe the earth at nine discrete angles; one at nadir plus eight other symmetrically placed cameras that provide fore-aft observations with view angles, at the earth's surface, of 26.1, 45.6, 60.0, and 70.0° relative to the local vertical. Each camera contains four detector line arrays, each overlain by a spectral filter providing imagery at four spectral bands within the visible and near-infrared (NIR).

The purpose of flying an aircraft instrument, AirMISR, is to collect MISR-like data sets to support in the development and validation of MISR data products, and to provide a verification of the EOS-AM1 MISR sensor calibration. It is believed, however, that AirMISR data will enable scientific research irrespective of MISR, in that program objectives are to produce high-quality, well calibrated multi-angle imaging data sets.

The AirMISR instrument flies on an ER-2 aircraft, and collects data at an altitude of 20 km. Unlike the EOS MISR, which contains nine individual cameras pointed at discrete look angles, AirMISR utilizes a single camera in a pivoting gimbal mount. A schematic of the flight view-angle sequence is shown in Figure 1. The camera has been fabricated from MISR brassboard and engineering model components², and thus has similar radiometric and spectral response as the MISR cameras. Another difference between the MISR and AirMISR cameras is in the focal plane temperature. The MISR focal plane is temperature-stabilized at -5° C; whereas the AirMISR focal plane temperature is controlled by the Optical Mechanical Structure temperature controller at 20° C. The added dark current for the AirMISR camera is not sufficient to affect science performance.

2. SPECTRAL CALIBRATION

During MISR spectral calibration, the response profile was measured at three field positions and for nine cameras, for each of the four spectral bands. These data were found to be similar enough, and an averaged profile was adopted. These "Standardized spectral response profiles" are reported within the Ancillary Radiometric Product (ARP), a data file used in MISR standard product production. Data are from 365 to 1100 nm, in 0.5 nm steps, with a spectral resolution of 2.6 nm for the in-band region, and 19.6 nm otherwise. The spectral parameters quoted for MISR result from a solar-weighted, in-band moments analysis of the Standardized spectral response profiles. These parameters are 446.3, 557.5, 671.8, and 866.5 nm for center wavelength, and 40.9, 27.2, 20.4, and 38.6 nm for bandwidth.

The same laboratory facilities and procedures³ used for MISR calibration have been used for AirMISR calibration. Though measured spectral response data are available, AirMISR data product generation will make use of the MISR standardized

parameters. It is believed the simplification to processing outweighs any slight advantage to be gained in using the original measurements. A comparison between the standardized values and those measured specifically on the AirMISR camera are given in Table 1. The MISR out-of-band responses are listed for the range of values found within the nine cameras. AirMISR Band 3/ Red is shown to have an out-of-band response twice that of any MISR camera. It is noted that this focal plane was deliberately bypassed during the MISR build, in that better performance was found on alternate units. The measured AirMISR spectral scans are shown in Figures 2-5, and highlight the out-of-band leak in the Red Band. The dashed line at the 0.001 level of transmittance represents the MISR specification on peak out-of-band transmittance. The dashed line at 0.0001 represents the specification on out-of-band, averaged over 100 nm intervals.

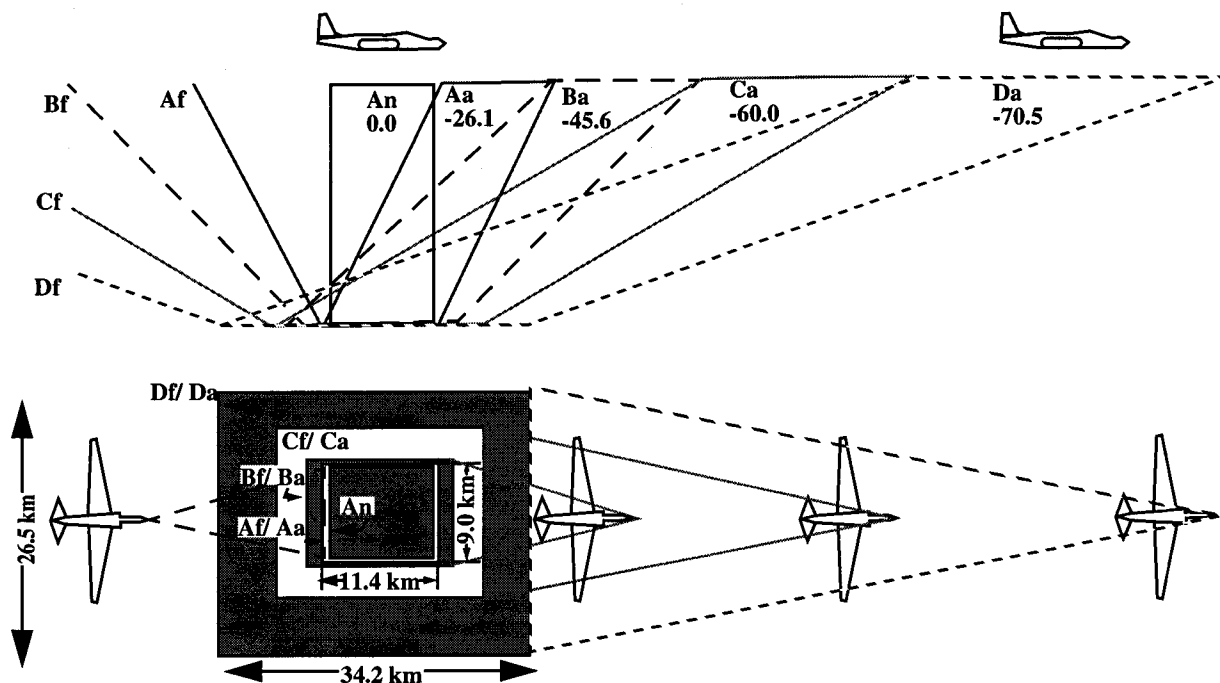


Figure 1. AirMISR gimbal scheme used to acquire data at nine view angles.

Table 1. A comparison of MISR/ AirMISR spectral parameters

Parameter	MISR standardized values				AirMISR measured values			
	Band 1	Band 2	Band 3	Band 4	Band 1	Band 2	Band 3	Band 4
In-band, moments analysis center wavelength, nm	446.3	557.5	671.8	866.5	447.1	558.8	671.8	866.7
In-band, moments analysis spectral bandwidth, nm	40.9	27.2	20.4	38.6	44.3	28.7	21.0	39.1
Total-band, moments analysis center wavelength, nm	447.5	557.8	669.5	857.8	448.4	559.6	666.7	860.8
Total-band, moments analysis spectral bandwidth, nm	69.5	74.5	91.9	184.2	76.8	76.6	138.5	153.2
Out-of-band response, %	1	2-3	2	0.8-2	0.87	2.32	4.92	1.80

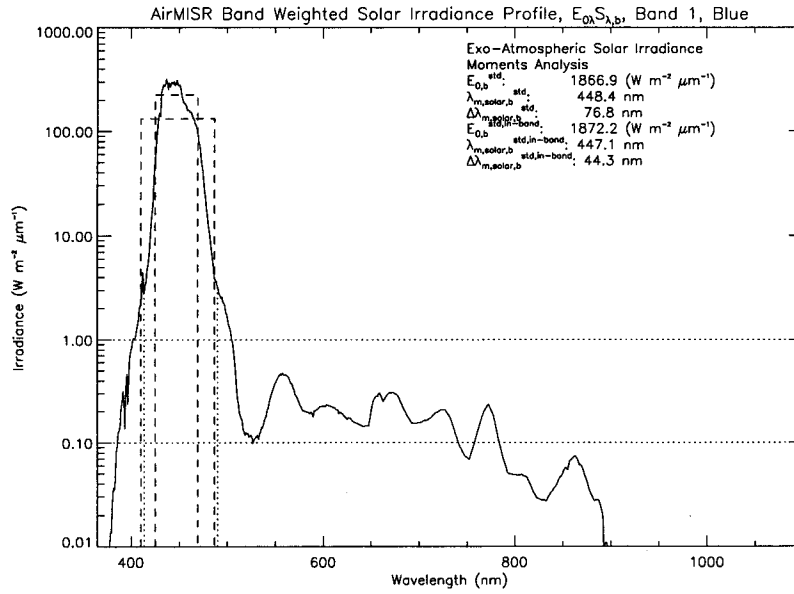


Figure 2. AirMISR measured spectral response profile for Band 1/ Blue.

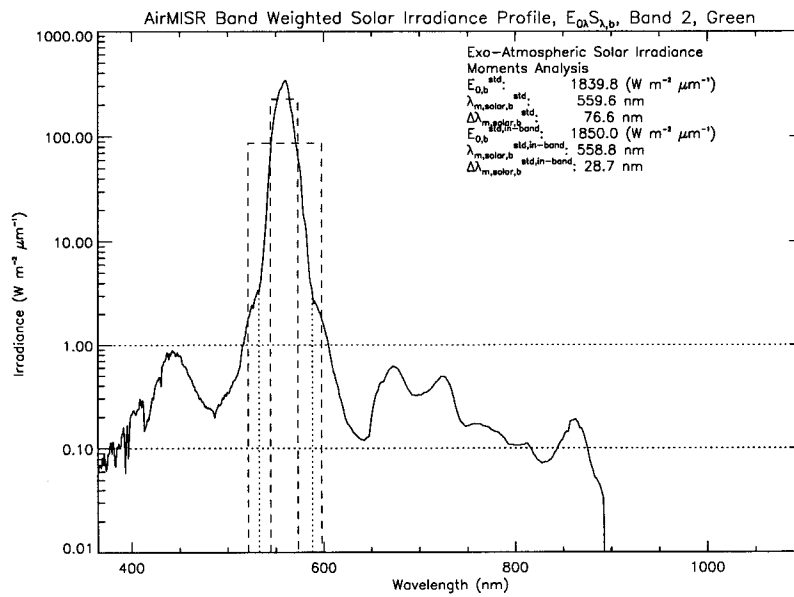


Figure 3. AirMISR measured spectral response profile for Band 2/ Green.

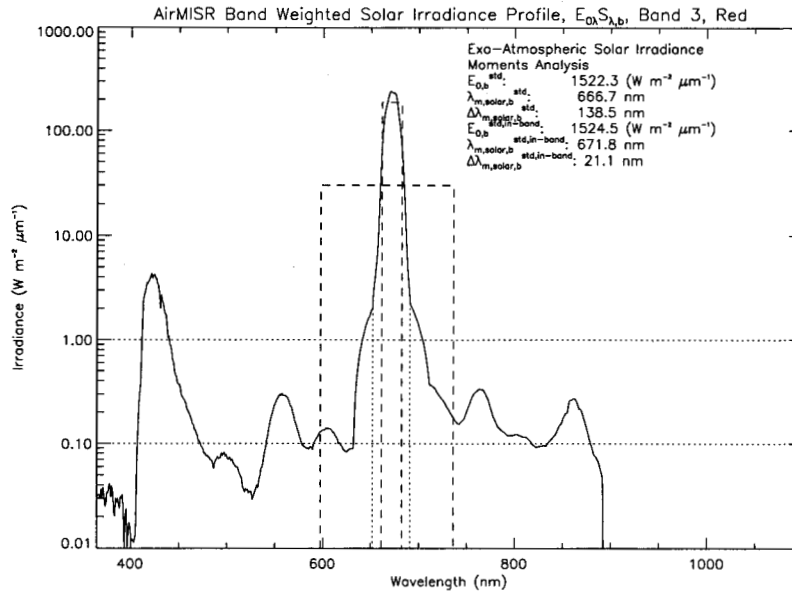


Figure 4. AirMISR measured spectral response profile for Band 3/ Red.

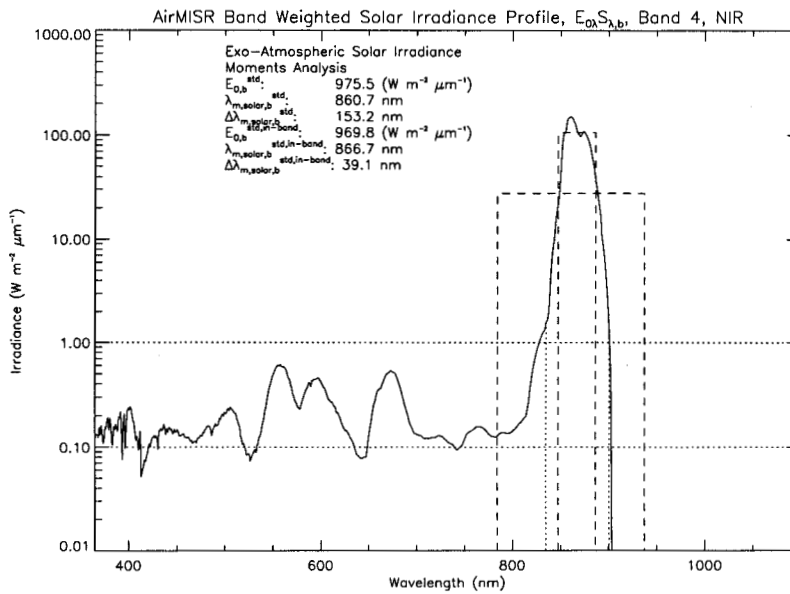


Figure 5. AirMISR measured spectral response profile for Band 4/ Near-infrared.

3. RADIOMETRIC CALIBRATION

The radiometric calibration of AirMISR is again accomplished by using heritage from the MISR program³. A 1.65 m (65") integrating sphere, with an exit aperture of 23 x 76 cm (9 x 30") is used for the flat-field source. This aperture, which fits over the 76 cm (30") circular sphere exit port, is used to minimize multiple reflections between the AirMISR or MISR cameras and the sphere exterior. Whereas MISR has been calibrated in a vacuum chamber, AirMISR has been calibrated at ambient pressure. This relaxation in the procedures is allowed in that the flight AirMISR focal plane temperature is approximately that of the

clean-room ambient temperature. No ambient-vacuum filter shifts occur with AirMISR (or MISR), as the focal planes are hermetically sealed.

The sphere output is placed on a radiometric scale by measurements made with detector standards. A QED-200 (made of United Detector Technology inversion layer diodes) is used to measure sphere output for the blue and green MISR spectral bands, Bands 1 and 2; and a QED-150 (made of Hamamatsu p-on-n photodiodes) is used for the red and near-infrared channels, Bands 3 and 4. Each detector is nearly 100% in internal quantum efficiency, for the wavelength regions at which they are operated, and is mounted in a light-trap configuration so as to collect the light reflected at each air/ detector interface. These standards are used with filters of the same spectral bandpass design as the flight cameras, and with a known field-of-view, established by use of a precision aperture tube. Traceability to Système International (SI) units is established through the measurement protocols of current, apertures, and aperture distances. JPL maintains working standards of voltage, resistance, and length which are traceable to the National Institute of Standards and Technology (NIST) or other international standards that are recognized by NIST.

The radiometric calibration is performed using the specific CCD integration times that are to be used during flight. These are determined such that the signal-to-noise ratio (SNR) specifications are just met at the edge-of-field, where the system transmittance is smallest. This allows the greatest margin between detector saturation and scene radiance. These integration times can be changed should the AirMISR sensor degrade. A recalibration of the focal plane would follow. The nominal integration times for the upcoming flight season have been determined to be 13.44, 18.88, 25.60, and 21.76 msec for Band 1/ Blue through Band 4/ NIR, respectively. A maximum integration time of 40.8 msec is allowable for each band.

The radiometric equation used to convert AirMISR output DN to band-averaged radiance is given by:

$$G_2(\mathcal{L}^{\text{std}})^2 + G_1\mathcal{L}^{\text{std}} + G_0 = \text{DN} - \text{DN}_0 \quad (1)$$

where

- \mathcal{L}^{std} is the incident radiance, weighted by S_λ , the band-specific standardized response profile [$\text{W m}^{-2} \text{sr}^{-1} \mu\text{m}^{-1}$],
- DN is the camera digital number,
- G_2 , G_1 , and G_0 are best fit parameters to the measured radiative transfer curve, and
- DN_0 is the digital number associated with the video offset voltage, unique for each line of data, and measured by the overclock pixels for that line.

The channel averaged coefficients for AirMISR are presented in Table 2.

Table 2. AirMISR array-averaged radiometric gain coefficients.

Spectral Band	G_0 , DN	G_1 , DN/($\text{W m}^{-2} \text{sr}^{-1} \mu\text{m}^{-1}$)	G_2 , DN/($\text{W m}^{-2} \text{sr}^{-1} \mu\text{m}^{-1}$) ²
Band 1/ Blue	9.88	23.26	4.34e-4
Band 2/ Green	21.17	23.82	1.15e-4
Band 3/ Red	51.77	28.92	1.89e-3
Band 4/ NIR	7.81	46.98	3.643e-3

The radiometric uncertainties for this AirMISR laboratory calibration are the same as those reported for the MISR calibration⁴. All radiometric uncertainty specifications are believed to have been met for AirMISR. This includes a 3% absolute uncertainty (1σ) at an equivalent reflectance of 100% (that is near the upper end of the sensor response curve).

There are several pixels within the AirMISR focal plane that are less responsive than their neighbors. These pixels can be identified by plotting the flat-field response of the camera, as shown in Figures 6 and 7. In particular there is a region in both Band 1/ Blue and Band 2/ Green of about 10 pixels in width, centered at pixel 1408, in which the response drop exceeds 10%. Further, for four pixels in this region the response drop exceeds 50%. For these pixels the signal-to-noise ratio (SNR) of the camera is slightly smaller. For most pixels, however, the SNR specifications are met. Table 3 gives the array-averaged measured SNR as compared to the specification. The specification values listed here are interpolated from the illumination levels given in the original specifications document.

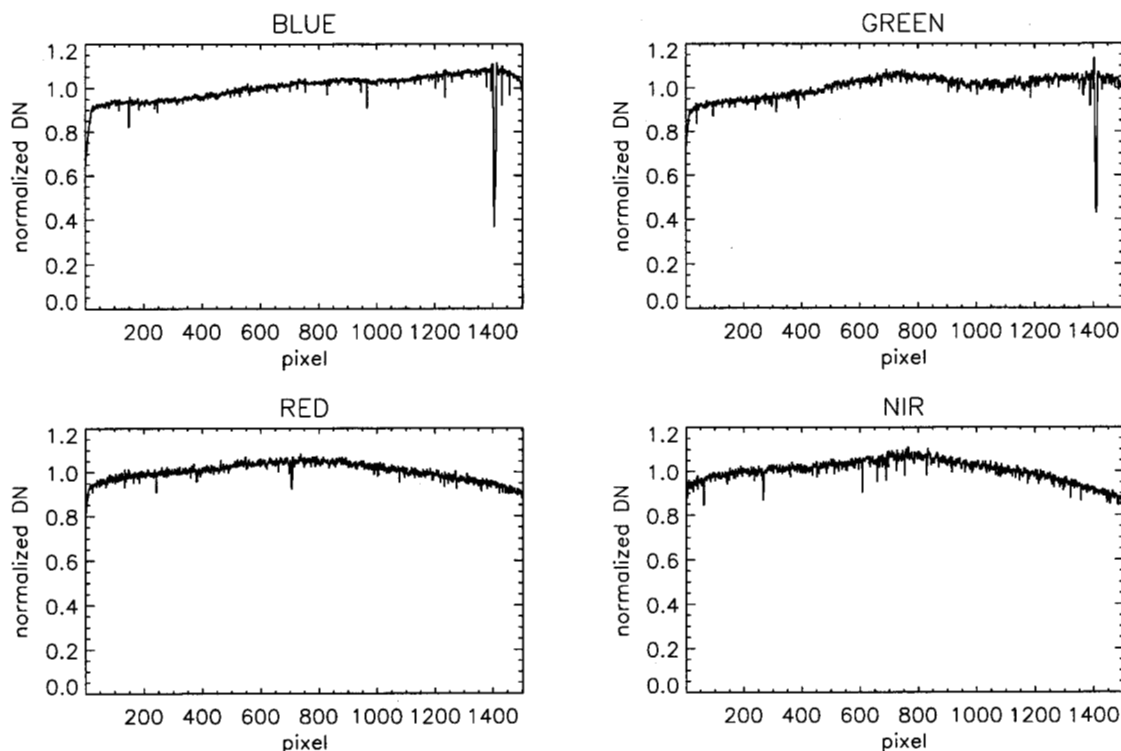


Figure 6. AirMISR response to a flat-field target.

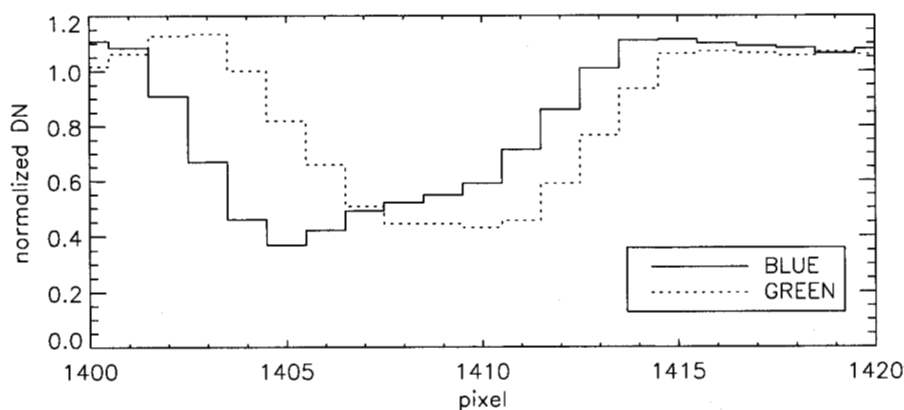


Figure 7. Low response region of AirMISR response to a flat-field target for Band 1/Blue and Band 2/Green.

In Figures 6 and 7, normalized DN refers to the ratio of the data number (DN) for a given pixel to the average DN for the line, i.e., the average over all 1504 pixels.

Table 3. Band-averaged signal-to-noise ratios for AirMISR.

Spectral band	Test illumination: target equivalent reflectance level	SNR	
		Specification	Measured array mean and standard deviation
Band 1/ Blue	35.2%	376	759±74
Band 2/ Green	83.7%	646	969±91
Band 3/ Red	97.9%	693	775±74
Band 4/ NIR	104.8%	700	705±70

Figure 8 is an AirMISR nadir image of Moffett field shown as raw DN. The low response pixel region appears as a dark stripe in the image. It was acquired on 5 November 1997 at 10:55:23 AM.



Figure 8. Band 2/Green DN image from AirMISR file An.Run.971105.105523 (1504 pixels x 1081 lines), illustrating the appearance of the low response pixel region.

The low response regions are of interest because the application of the calibration coefficients does not completely correct the image in these regions as illustrated by Figure 9. An examination of the residuals from the radiometric calibration data which were used to derive the calibration coefficients shows the fit to be no better nor worse for a pixel in the low response region than for other pixels in the array outside of this region. The increased uncertainty in the retrieved radiance is not that the low response pixels do not fit the quadratic model. The pixels in the low response region exhibit a larger Noise Equivalent Change in Reflectance ($NE\Delta\rho = \rho/SNR$) than the surrounding pixels. They have a reduced radiometric sensitivity due to increased

noise. A one DN change in signal maps to a larger change in radiance for the low response regions of Band 1/Blue and Band 2/Green. This is illustrated in Figure 10, which shows the inverse of the linear fit parameter, G_1 , in the low response pixel region. The linear term is the dominant factor in the radiometric equation (1).

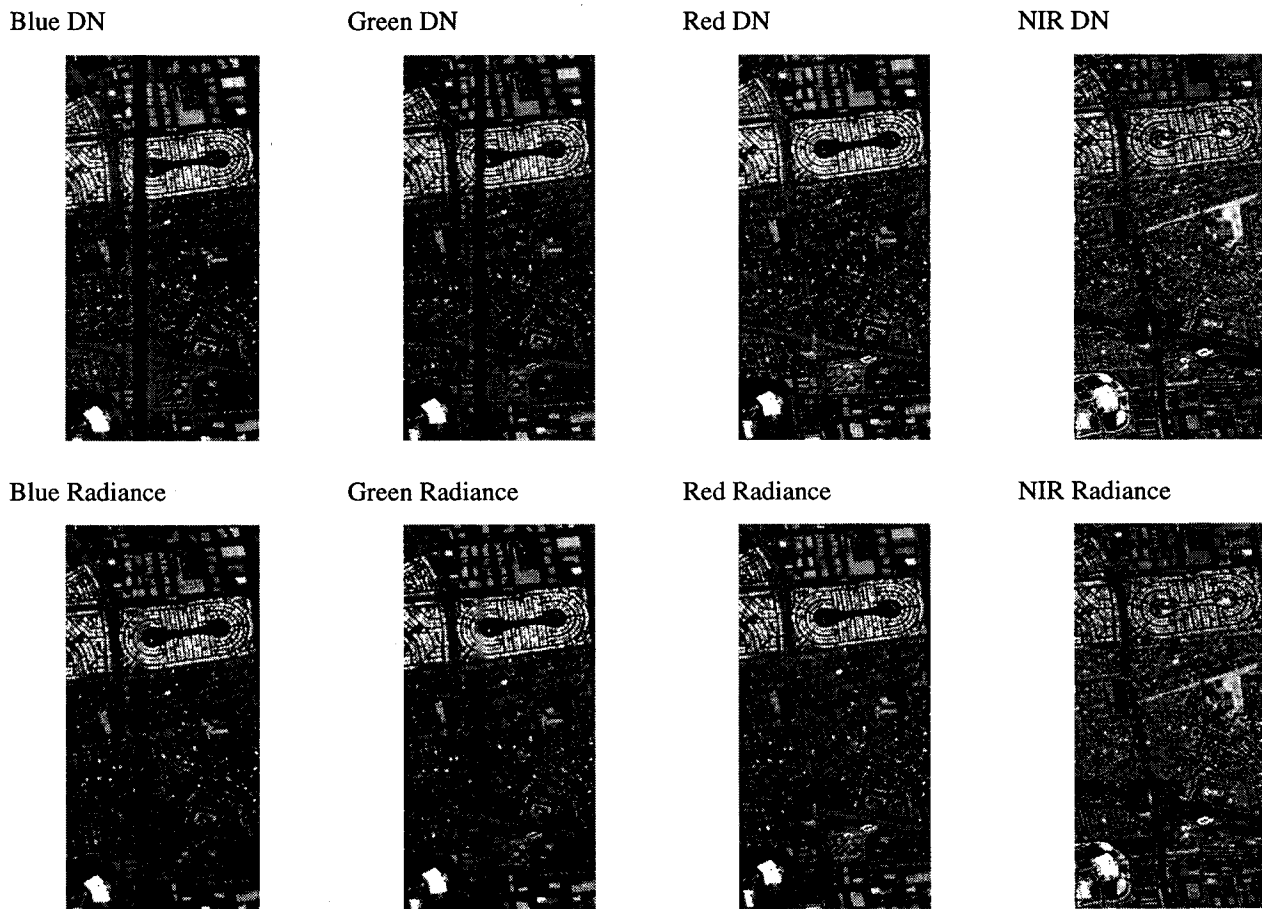


Figure 9. Pixels 1351-1500, Lines 501-800 of An.Run.971105.105523, DN and Radiance.

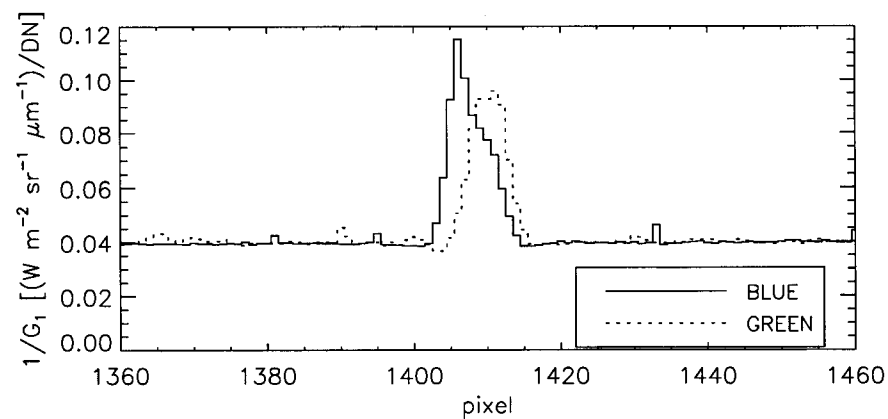


Figure 10. Inverse of the linear fit parameter, G_1 , for Band 1/Blue and Band 2/Green.

4. CONCLUSIONS

The AirMISR camera strongly reflects its MISR heritage: it was built and calibrated to the same standards as the nine cameras that comprise MISR. Being an aircraft instrument, AirMISR can be brought back to the laboratory in order to update the radiometric calibration on a regular basis. The AirMISR radiometric calibration will also be verified with vicarious calibration. In Figure 11, the asterisk symbols represent radiance values from a vicarious calibration experiment, the details of which will be published elsewhere⁵, and the solid line represents the radiances derived from the laboratory coefficients. Agreement is found to be quite good.

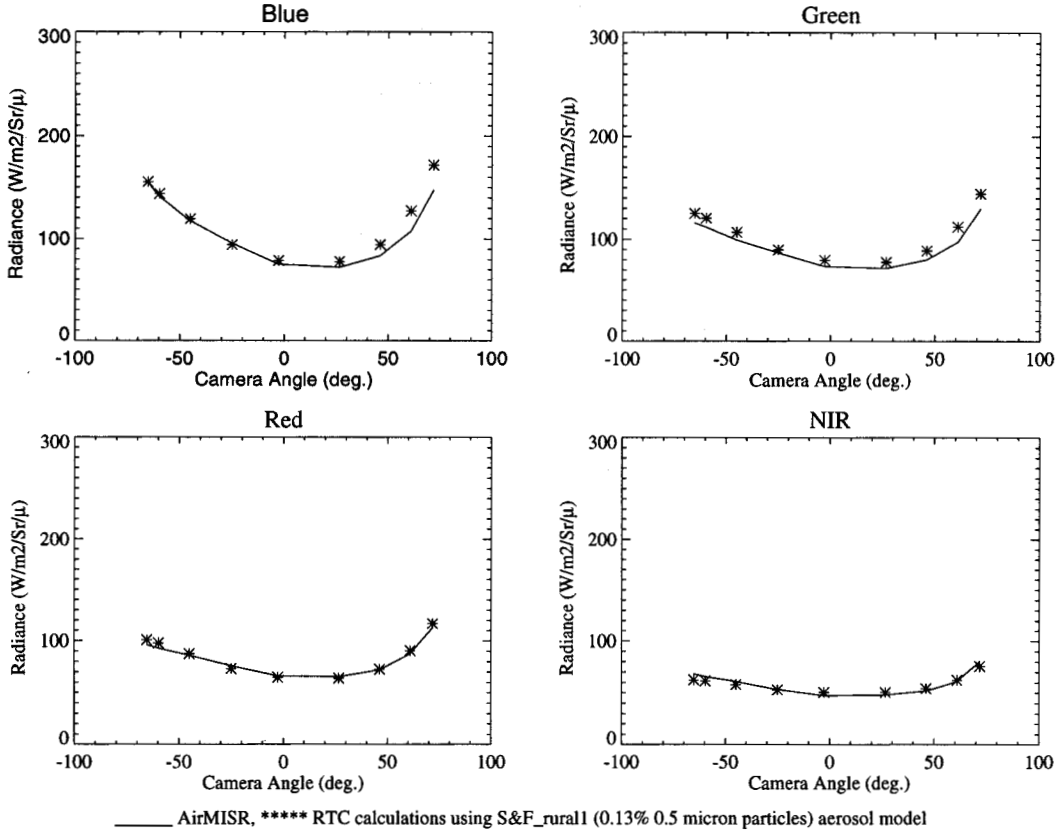


Figure 11. Comparison of AirMISR laboratory and vicarious calibrations.

5. ACKNOWLEDGMENTS

The design, calibration, and operation of AirMISR is attributed to a great number of individuals. David J. Diner is the Principal Investigator for MISR and AirMISR, and has defined the science performance requirements, data products, and experiment concept. Thomas G. Chrien, Charles M. Sarture and Charles G. Kurzweil were key players in the design of AirMISR. Jose Garcia, the AirMISR electrical engineer, was responsible for the acquisition of the laboratory calibration data presented here. He was assisted by Ghobad Saghri and Daniel Preston, MISR calibration engineers. James E. Conel is responsible for the AirMISR mission planning, and Mark C. Helmlinger acquired the in-situ measurements used to produce the vicarious calibration results. William C. Ledebor has defined and produced the AirMISR radiometric products, and has assisted in evaluating AirMISR image data used for the vicarious calibration study. Stuart H. Pilorz and Wedad A. Abdou are responsible for much of the algorithm development and analyses utilized in the vicarious calibration experiments. The work described in this paper is being carried out by the Jet Propulsion Laboratory, California Institute of Technology, under contract with the National Aeronautics and Space Administration.

6. REFERENCES

1. Diner, D.J., J.C. Beckert, T.H. Reilly, C.J. Bruegge, J.E. Conel, R. Kahn, J.V. Martonchik, T.P. Ackerman, R. Davies, S.A.W. Gerstl, H.R. Gordon, J-P. Muller, R. Myneni, R.J. Sellers, B. Pinty, and M.M. Verstraete (1998). Multiangle Imaging SpectroRadiometer (MISR) description and experiment overview. *IEEE Trans. Geosci. Rem. Sens.*, Vol. 36, 1072-1087.
2. Diner, D.J., L.M. Barge, C.J. Bruegge, T.G. Chrien, J.E. Conel, M.L. Eastwood, J.D. Garcia, M.A. Hernandez, C.G. Kurzweil, W.C. Ledebor, N.D. Pignatano, C.M. Sarture, and B.G. Smith (1998). The Airborne Multi-angle SpectroRadiometer (AirMISR): instrument description and first results. *IEEE Trans. Geosci. Rem. Sens.*, Vol. 36, pp. 1339-1349.
3. Bruegge, C.J., V.G. Duval, N.L. Chrien, R.P. Korechoff, B.J. Gaitley, and E.B. Hochberg (1998). MISR prelaunch instrument calibration and characterization results. *IEEE Trans. Geosci. Rem. Sens.*, Vol. 36, pp. 1186-1198.
4. Bruegge, C.J., N. L. Chrien, R. A. Kahn, J. V. Martonchik, David Diner (1998). Radiometric Uncertainty Tabulations for the Retrieval of MISR Aerosol Products. Conference issue: New Developments and Applications in Optical Radiometry (NEWRAD '97), *Metrologia*. In press.
5. Abdou, W.A., C.J. Bruegge, M.C. Helmlinger, B.J. Gaitley, W.C. Ledebor, S.H. Pilorz, J.E. Conel, and J.V. Martonchik (1998). Vicarious reflectance-based absolute radiometric calibration of AirMISR. *Remote Sens. of Environment*, in preparation.